Development 135, 513-521 (2008) doi:10.1242/dev.010876

Drosophila Activin-β and the Activin-like product Dawdle function redundantly to regulate proliferation in the larval brain

Changqi C. Zhu[1], Jason Q. Boone[2], Philip A. Jensen[1], Scott Hanna[3], Lynn Podemski[3], John Locke[3], Chris Q. Doe[2,4] and Michael B. O'Connor[1,5,*]

The *Drosophila* Activin-like ligands Activin-β and Dawdle control several aspects of neuronal morphogenesis, including mushroom body remodeling, dorsal neuron morphogenesis and motoneuron axon guidance. Here we show that the same two ligands act redundantly through the Activin receptor Babo and its transcriptional mediator Smad2 (Smox), to regulate neuroblast numbers and proliferation rates in the developing larval brain. Blocking this pathway results in the development of larvae with small brains and aberrant photoreceptor axon targeting, and restoring *babo* function in neuroblasts rescued these mutant phenotypes. These results suggest that the Activin signaling pathway is required for producing the proper number of neurons to enable normal connection of incoming photoreceptor axons to their targets. Furthermore, as the Activin pathway plays a key role in regulating propagation of mouse and human embryonic stem cells, our observation that it also regulates neuroblast numbers and proliferation in *Drosophila* suggests that involvement of Activins in controlling stem cell propagation may be a common regulatory feature of this family of TGF-β-type ligands.

KEY WORDS: Activin, Brain, *Drosophila*, Larvae, Optic lobe, Proliferation

INTRODUCTION

The TGF-β family of growth and differentiation factors controls a wide range of developmental processes including early axis specification, cell proliferation, apoptosis, differentiation and stem cell propagation (Massague et al., 2000). These factors bind to a heteromeric receptor complex containing type I and II transmembrane serine/threonine kinases. Upon ligand binding, the type I receptor kinase is activated by the type II receptor and phosphorylates members of the R-Smad family of transcription factors. TGF-β signaling pathways are broadly divided into either the BMP or Activin/TGF-β branches, based on which Smad transcription factors they phosphorylate (Feng and Derynck, 2005). The BMP family of ligands signal through R-Smads1/5/8 whereas the Activin/TGF-β branch utilizes R-Smads2/3. Phosphorylation of R-Smads facilitates their association with a common Co-Smad and retention of the R-Smad–Co-Smad complex in the nucleus, where it regulates transcription of target genes in association with a wide variety of co-factors (Miyazono et al., 2006).

Drosophila employs both BMP and Activin-like signaling pathways to regulate numerous developmental processes. Among the seven TGF-β type ligands, Decapentaplegic (Dpp), Screw (Scw), and Glass bottom boat (Gbb) are members of the BMP family, whereas Activin-β (Actβ) and Dawdle (Daw) (Parker et al., 2004; Serpe and O'Connor, 2006), fall within the Activin/TGF-β branch. Two novel ligands, Maverick (Mav) and Myoglianin, are sufficiently diverged to preclude clear assignment to a particular ligand subfamily (Parker et al., 2004). Both the BMP and Activin/TGF-β pathways employ Punt as a common type II receptor, and pathway specificity is provided by the type I receptors (Brummel et al., 1999; Brummel et al., 1994; Das et al., 1999; Letsou et al., 1995; Ruberte et al., 1995; Serpe and O'Connor, 2006; Zheng et al., 2003). Tkv and Sax bind BMP-type ligands and phosphorylate Mad, whereas Babo binds Activin-like ligands and signals through Smad2 (also known as Smox – FlyBase) (Das et al., 1999; Serpe and O'Connor, 2006; Shimmi et al., 2005a; Shimmi et al., 2005b; Zheng et al., 2003).

Parsing out the functional relationship between individual TGF-β ligands and receptors and particular developmental processes is a difficult process, especially in vertebrates, in which the numbers of ligands and receptors are large. In general, this process involves biochemically matching a particular ligand with one or more signaling receptors and comparing the phenotypes produced by knockdown of the different signaling components. In *Drosophila*, the contributions of BMP pathway components to numerous developmental processes, including cell-fate specification, imaginal-disc growth and patterning and synapse development, have been well studied (reviewed by Parker et al., 2004). By contrast, the Activin pathway is less well characterized. Unlike mutations in the BMP pathway, mutations in Activin signaling components have not been shown to directly affect differentiation but instead appear to primarily regulate neuronal wiring and proliferation. For example, clonal analysis of either *babo* or *Smad2* mutants has shown that this pathway regulates mushroom body remodeling during metamorphosis (Zheng et al., 2003), morphogenesis of ellipsoid body neurons in the adult (Zheng et al., 2006) and motor axon guidance in the embryo (Parker et al., 2006; Serpe and O'Connor, 2006). Regarding proliferation, loss of both maternal and zygotic *babo* leads to small brains and small but properly patterned wings (Brummel et al., 1999), indicating a potential role in regulating proliferation of larval mitotic tissue.

[1]Department of Genetics, Cell Biology and Development, Howard Hughes Medical Institute, University of Minnesota, 6-160 Jackson Hall, Minneapolis, MN 55455, USA. [2]Institute of Neuroscience, Howard Hughes Medical Institute, University of Oregon, Eugene, OR 97403, USA. [3]Department of Biological Sciences, University of Alberta, Alberta, T6G 2E9, Canada. [4]Howard Hughes Medical Institute, University of Oregon, Eugene OR 97403, USA. [5]Howard Hughes Medical Institute, University of Minnesota, 6-160 Jackson Hall, Minneapolis, MN 55455, USA.

*Author for correspondence (e-mail: moconnor@umn.edu)

Accepted 29 October 2007

Analysis of *Drosophila* Actβ and Daw ligand loss-of-function phenotypes indicates that these two ligands probably regulate separate aspects of neuronal wiring, as dominant-negative and RNAi constructs that reduce the activity of *actβ* phenocopy the mushroom body remodeling defects seen in *babo* and *Smad2* mutants (Zheng et al., 2003), whereas null mutants of *daw* phenocopy the *babo* and *Smad2* mutant motor axon guidance defects (Parker et al., 2006; Serpe and O'Connor, 2006). In neither case, however, was an obvious proliferation defect reported for loss of either ligand.

In this paper, we investigate the role of the *Drosophila* Babo/Smad2 pathway in larval brain development. We show that mutations in *babo* and *Smad2* result in small brains with altered innervation of photoreceptor axons within the lamina and medulla. In contrast to the wiring defects described above, however, we demonstrate that these aberrations are not caused by defects in photoreceptor innervation or changes in cell fate of target neurons within the brain. Instead, they result primarily from reduced proliferation within the optic lobe and central brain leading to a reduction in the size of the photoreceptor target field. We further demonstrate that the Babo receptor is required in neuroblasts and that the ligands Actβ and Daw function redundantly to control proliferation in the brain. These results suggest that while the two *Drosophila* Activin-like ligands have at least partially independent roles in regulating neuronal wiring, they have largely redundant roles in regulating proliferation within the brain.

MATERIALS AND METHODS

Drosophila genetics

The strong loss-of-function *babo* alleles, $babo^{32}$, $babo^{52}$ and $babo^{26}$, have been described previously (Brummel et al., 1999), as has the strong $Smad2^{mb388}$ allele (Zheng et al., 2003). Previously, we reported that $babo^{32}$ homozygotes have very low levels of BrdU incorporation in third-instar brains (Brummel et al., 1999). However, we have since found that the $babo^{32}$ chromosome contains a second hit, which when homozygous leads to developmental delay and severely reduced cell proliferation (M.B.O., unpublished). Therefore, only heterozygous combinations of *babo* alelles are used in these studies. The daw^{ex32} and daw^{ex11} are strong and moderate loss-of-function alleles, respectively (Serpe and O'Connor, 2006), whereas daw^{4} is a presumed null mutation (Parker et al., 2006). The *Cyclin* A^{c8LR1} allele is a strong amorph (Sigrist and Lehner, 1997) and was obtained from the Bloomington Stock Center. For genetic rescue experiments, *babo* mutant lines carrying various Gal4 drivers were crossed to different *babo* mutant alleles carrying UAS transgenes. The 1407>Gal4 driver (Luo et al., 1994) was obtained from K.-F. Fischbach and the *worniu*>Gal4 has been previously described (Albertson et al., 2004). The *da*>Gal4, *elav*>Gal4, and *ey*>Gal4 lines were obtained from the Bloomington Stock Center. Mutant *babo* alleles with different Gal4 drivers and UAS transgenes were balanced by the Cy^{O}*::Tm6,Tb* compound chromosome. Null *babo* photoreceptor clones were generated by crossing *FRTG13babo*^{52}/Cy^{O}*::Tm6,Tb* flies to *FRTG13uasCD8GFP; eyGal4-uasFlp*/Cy^{O}*::Tm6,Tb* flies. GFP-positive MARCM clones were induced by heat shock at 36°C for 1 hour of early second-instar larvae from the cross of *elavGal4hsFlp; FRTG13tubGal80*/Cy^{O} and *FRTG13babo*^{w224}*UASmCD8GFP*/Cy^{O}. To identify *daw, actβ* double mutants, non-GFP, *y* larvae were obtained from the stock *daw*/Cy^{O}, actin-GFP; $act\beta^{ed80}$/Dp1:4 (*y*+, *spa*). All crosses were done at 25°C.

The *daw* promoter-Gal4 line was generated by cloning a 9 kb PCR fragment containing the first intron and upstream sequences using the following primer pair 5′-CTGAGCCCCTACGTCTGTATGATATG-3′ and antisense 5′-GATCTTCTGGATCGCCTTTGGTTTCA-3′ into the pPelicanGal4 plasmid, which is derived from pPelican (Barolo et al., 2000). Transgenic flies were generated by standard injection procedure.

Staging of larvae

Freshly hatched larvae were collected for 5 hours on apple-agar plates and staged to white prepupal stages (120 hours for *yw* and 144 hours for *babo* mutants).

Immunostaining

Larval brain lobes, together with imaginal discs, were dissected in PBS and fixed in 3.7% formaldehyde in PBS for 1 hour at room temperature, and were washed by PBS plus 0.1% Triton X-100 (PBT). Antibodies purchased from the Developmental Studies Hybridoma Bank (DSHB) include mouse 24B10 (1/100 dilution), rat anti-Elav (7E8A10, 1/400), mouse anti-Dachshund (mAbdac2-3, 1/50), mouse anti-Robo 13C9, (1/50), mouse anti-Repo 8D12, (1/50 dilution), mouse anti-BrdU G3G4 (1/100), anti-Arm 7A1 (1/500), mouse anti-Pros MR1A (1/100) and mouse anti-Discs large (1/1000). Rabbit anti-phosphorylated histone H3 ($pSer^{10}$, H-0412) was from Sigma (1/400). Rabbit anti-Cyclin A antibody was used at 1/500 dilution (Whitfield et al., 1990; Nakato et al., 2002). Rabbit anti-Scrib was diluted at 1:2500 (Albertson et al., 2004), and guinea-pig anti-Mira at 1:500 (Lee et al., 2006). Anti-active Caspase-3 antibody was a gift from Idun Pharmaceuticals, and used at 1/2000 dilution. Rat monoclonal N-Cadherin antibody, DUex8, was a gift from L. Zipursky and was used at a 1/50 dilution. Fluorescent conjugated secondary antibodies (Molecular Probes) were used at 1/200 dilution. All primary antibodies were diluted in PBT and incubated with tissue samples at 4°C overnight. Secondary antibodies were typically incubated with tissue samples for 2 hours at room temperature. Confocal images were taken with a Zeiss Axio confocal microscope or a Leica TCS SP2.

BrdU incorporation

Larval brain lobes and attached eye discs were dissected in PBS and transferred to M3 complete medium containing 0.4 mg/ml BrdU (Roche) and incubated at 25°C for 30 minutes before fixation. Fixed tissue was treated in 2 N of HCl at room temperature for 30 minutes before the addition of anti-BrdU monoclonal antibody.

RESULTS

Babo and Smad2 are required for proper retinal axon targeting

Previous work has implicated the Babo/Smad2 pathway in proper morphogenesis of several larval and adult brain neurons (Zheng et al., 2003; Zheng et al., 2006). We noticed that mutant third-instar larvae also showed variable defects in photoreceptor innervation of the lamina and medulla (Fig. 1A vs B). Differentiated photoreceptor cells are normally organized as ommatidial units, each consisting of eight photoreceptor cells, R1-R8, which send their axons through the optic stalk into developing optic lobes. The axons of R1-R6 terminate and form a neural plexus at the lamina, whereas the axons of R7 and R8 project to the medulla (Clandinin and Zipursky, 2002) (Fig. 1A). In *babo* mutant brains, photoreceptors R1-6 formed a lamina plexus that was very reduced in size (Fig. 1B). In addition, the R7 and R8 axon projections to the medulla were highly perturbed, and their growth cones formed bundles instead of a regular lattice network typical of controls (Fig. 1A vs 1B insets). This defect was not corrected at later stages, as axon targeting was still highly perturbed in 3-day-old *babo* mutant pupae, and rotation of the medulla and lamina relative to one another did not take place (Fig. 1D vs E). *Smad2* mutants exhibited similar photoreceptor axon targeting defects, indicating that the *babo* defect is caused by the loss of the canonical Activin signaling pathway (Fig. 1C).

To further characterize the *babo* phenotype, we also immunostained *babo* mutant brain lobes with anti-Dachshund (Dac) antibody to highlight lamina neuron precursor cells, and with anti-Elav to visualize differentiated neurons. In the most severe cases, *babo* mutants exhibited reduced numbers of lamina cap neurons (Fig. 2A vs B) and loss of Dac-positive cartridge neurons. In larvae with less severe phenotypes, the number of Dac-positive cells in each cartridge was not greatly different from

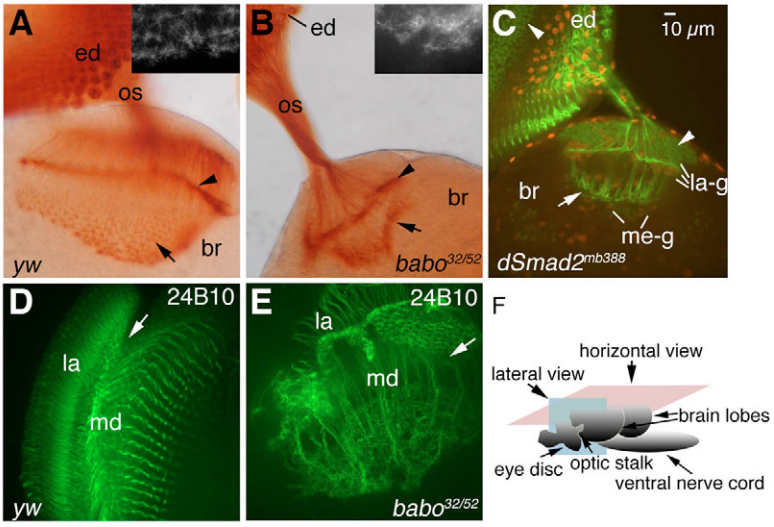

Fig. 1. *babo* mutants exhibit a severe defect in photoreceptor axon targeting. (**A**) Wild-type *yw* photoreceptor axon projections in a late third-instar *Drosophila* larva are highlighted by staining with antibody 24B10. The growth cones of R1-R6 form a neural plexus (arrowhead) at the lamina. R7 and R8 axons project to the medulla with individual growth cones forming a lattice-like array (arrow). Structures of individual growth cones of R7/R8 are illustrated with higher magnification in the inset. (**B**) An early white prepupa of *babo*$^{32/52}$ mutant (same magnification as A) showing a smaller brain lobe, reduced lamina plexus (arrowhead), abnormal R7/R8 photoreceptor axon projections (arrow) and bundled growth cones (inset). (**C**) A late third-instar *Drosophila Smad2* (*dSmad2*^{mb388}) mutant larva displaying photoreceptor axon (green, 24B10) targeting defects similar to those of *babo* mutants. Glia cells are stained by an anti-Repo antibody (red), and Dachshund antibody labeled the lamina neuron precursor cells (green, arrowhead) in the brain lobe and photoreceptor precursor cells in eye discs (also green, arrowhead). (**D**) A wild-type day 3 pupa showed normal turning (arrow) of R7/R8 axons (stained with 24B10) between lamina and medulla and a very well spaced array of R7/R8 axons in the medulla. (**E**) A day 3 *babo*$^{32/52}$ pupa showing lack of turning (arrow) and highly disorganized photoreceptor axons. (**F**) A schematic graph shows *Drosophila* central nervous system of a late third-instar larva with eye disc. Most images in this paper are horizontal confocal optic sections unless otherwise stated. br, brain lobes; ed, eye disc; la, lamina; md, medulla; os, optic stalk.

that seen *yw* controls, but the total number of lamina cartridges in *babo* mutants is smaller than that in wild type (see Fig. S1C in the supplementary material).

The severe aberrations of R7 and 8 termini in the medulla neuropil, which is composed in part by axons projecting from the lobula cortex, suggested that organization of this target field is probably disrupted. Consistent with this view, we find that babo mutants show a disorganized and smaller medulla neuropil compared with wild type, as revealed by anti-Robo (Fig. 2C vs D) which concentrates in the medulla axons derived from the lobular cortex neurons (Tayler et al., 2004). In addition, anti-N-Cadherin, which stains both photoreceptors and the medulla neuropil (Lee et al., 2001), also reveals a disruption in the medulla neuropil formation (Fig. 2G,I vs H-J).

Glial cells have been implicated as intermediate targets for photoreceptor axon targeting (Clandinin and Zipursky, 2002). Therefore, we examined *babo* and *Smad2* mutants with the glia-specific Repo antibody and compared them to *yw* controls. White prepupae of wild-type larvae showed three layers of well-aligned glial cells at the lamina and evenly distributed glia at the medulla cortex (Fig. 2E). By contrast, *babo* and *Smad2* mutants exhibited a reduced number of glia, with some misalignment of the glial cells within both the lamina and medulla (Fig. 1C and Fig. 2F).

Although based on only a limited number of markers, our data suggest that differentiation of neurons and glia is not grossly disrupted in the optic lobe of *babo* and *Smad2* mutants, raising the possibility that the observed retinal axon targeting defects may result from the production of fewer lamina and medulla progenitor cells within the optic lobe (see below).

Babo function is required in the optic lobe and not in photoreceptor axons

As *Drosophila* retinal axons have been shown to regulate proliferation in the lamina via delivery of Hedgehog and the EGF-like ligand Spitz to the target field (Huang and Kunes, 1996; Huang and Kunes, 1998; Huang et al., 1998), and because *Drosophila* Activin is expressed in photoreceptors (see Fig. S1A in the supplementary material), we wished to address whether *babo* function is required in photoreceptor axons or the brain for proper photoreceptor axon targeting and optic lobe development.

The *babo* gene is alternatively spliced, producing two protein isoforms, Babo$_a$ and Babo$_b$, which differ in their extracellular ligand-binding domain (Wrana et al., 1994). The babo$_a$ isoform has been specifically implicated in mushroom body remodeling (Zheng et al., 2003), while ectopic expression of either the Babo$_a$ or Babo$_b$ isoform rescues dorsal neuron morphogenesis defects of *babo* mutants. To examine the isoform requirements for proper optic lobe development and axon targeting, we expressed *babo$_a$* and *babo$_b$* individually or in combination using the ubiquitous *daughterless* Gal4 driver (*da*>Gal4). Expression of the *babo$_a$* isoform alone rescued neither the photoreceptor axon targeting nor brain size defects (Fig. 3B). By contrast, ubiquitous expression of *babo$_b$* alone (Fig. 3A) or *babo$_a$* and *babo$_b$* together (data not shown) not only rescued photoreceptor axon targeting and brain lobe defects, but also restored viability. These rescue data suggest that the *babo$_b$* isoform alone, at least when overexpressed, is sufficient to provide proper signaling activity for normal optic lobe development, axon targeting and viability.

To address tissue- and cell-type-specific requirements for *babo* function, a number of different Gal4 drivers were employed. Using the eye-specific driver *eyeless* Gal4 (*ey*>Gal4), we found that expression of neither *babo$_a$*, *babo$_b$* nor a combination of both in eye discs was able to rescue the *babo* mutant phenotype (Fig. 3C and data not shown). This suggested that *babo* function in the photoreceptors is not sufficient for directing normal photoreceptor axon targeting. We also used the FLP/FRT system to generate *babo* mutant clones in an otherwise *babo* heterozygous background. Large *babo*-mutant photoreceptor cell clones were found to project their axons normally into *babo* heterozygous brain lobes (Fig. 3E), providing further support for the argument that *babo* function in photoreceptor cells is dispensable for proper axon targeting and optic lobe development.

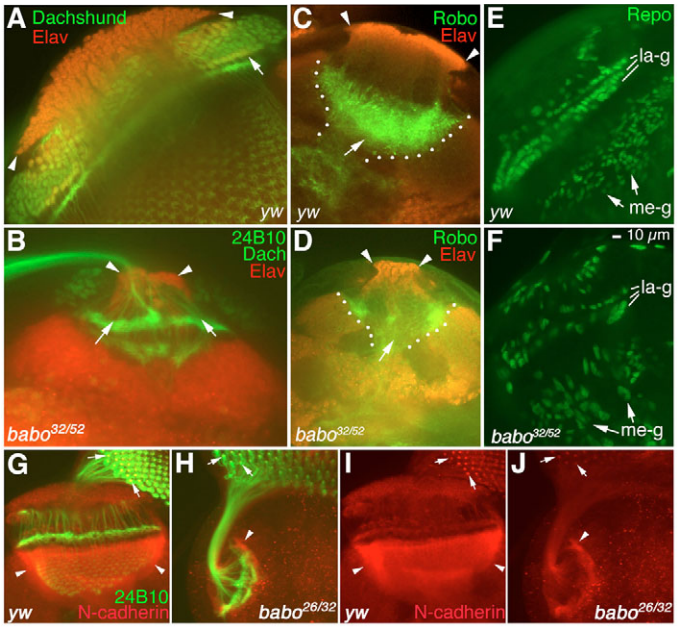

Fig. 2. Characterization of the optic lobe phenotypes of *Drosophila babo* mutants. (**A**) A wild-type *yw* white prepupa showed a large cap structure of lamina neurons (arrowheads) and lamina neuron precursor cells in the lamina cartridge (arrow). (**B**) The strongest $babo^{32/52}$ mutants have a very reduced number of lamina cap (arrowheads) and cartridge neurons (arrows), as revealed by Dachshund antibody (green) and Elav antibody (red) staining. (**C**) A wild-type *yw* wandering third-instar larva stained for Robo (green) and Elav (red). The arrowheads point to the lamina cap neurons, whereas the arrow points to the medulla neuropil (bracket of white dots). (**D**) A $babo^{32/52}$ mutant displayed a small lamina cap (arrowheads) and an aberrant medulla neuropil (arrow and white dots). (**E**) Normal distribution of glial cells labeled by repo antibody (green) in a brain lobe of a wild-type white prepupa. (**F**) A brain lobe of a $babo^{32/52}$ white prepupa, showing a reduced number of glial cells at both the lamina and medulla. (**G**,**H**) N-Cadherin (red) and 24B10 (photoreceptors green) staining of the optic lobe region from a *yw* white prepupae (G) and a $babo^{26/32}$ mutant (H). (**I**,**J**) The same images as G and H but red channel (N-Cadherin) only. Arrows mark photoreceptors and arrowheads the medulla neuropil. Note that overall intensity of N-Cadherin is not changed in either the photoreceptors or medulla neuropil, but the medulla neuropil is much smaller. la-g, glial cells at lamina; me-g, glial cells at medulla.

As glial cells provide both guidance cues and trophic factors for optic lobe development (Hidalgo et al., 2006), and because their numbers are reduced in *babo* mutants, we asked if selective expression of *babo* in glial cells was able to suppress any aspect of the *babo* mutant phenotype. As shown in Fig. 3D, expression of $babo_a$ and $babo_b$ in glial cells using the glia-specific driver *repo*>Gal4 did not alter the *babo* mutant phenotype. By contrast, expression of $babo_a$ and $babo_b$ using the 1407>Gal4 driver (Luo et al., 1994), which is expressed in both neuroblasts and many differentiating neurons of the brain but not in the eye disc (Fig. 3F), was able to rescue both brain size and the axon-targeting defect (Fig. 4G). In addition, the *worniu*>Gal4 driver that is expressed primarily in neuroblasts (Albertson et al., 2004) and ganglion mother cells (GMCs), but not the eye disc (Fig. 3H and see Fig. S3 in the supplementary material), was also able to rescue the *babo* mutant optic lobe phenotype (Fig. 3I), and some of these mutant animals survived to adults. Lastly, we found that overexpression of the EcR-1B receptor, the only known target of Actβ/$Babo_a$ signaling in the brain lobes, could not rescue the axon-targeting defects (data not shown) in contrast to its ability to suppress neuronal remodeling defects (Zheng et al., 2003; Zheng et al., 2006).

Taken together, these results suggest that, unlike the case for mushroom body remodeling and dorsal neuron morphogenesis or motor axon guidance, the failure of photoreceptors to properly innervate the lamina and medulla is not caused by an inability of these neurons to receive Babo/Smad2 signals or target cells to

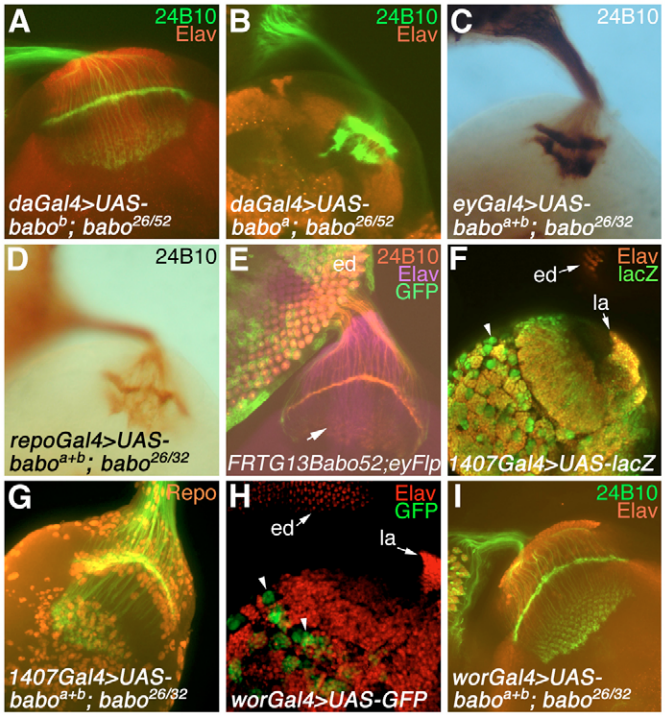

Fig. 3. Babo is required in the developing larval brain lobes but not in eye discs for normal photoreceptor axon targeting in *Drosophila*. Ubiquitous expression (*da*>Gal4) of UAS-$babo_b$ (**A**) but not the $babo_a$ (**B**) isoform rescues the photoreceptor axon targeting and small brain phenotype of $babo^{26/52}$ mutants. (**C**) No rescue of photoreceptor axon targeting phenotypes of $babo^{26/32}$ mutants by the expression UAS-$babo_{a+b}$ in eye discs (*ey*>Gal4 driver) or in glial cells (**D**, *repo*>Gal4). (**E**) $babo^{52}$ homozygous mutant photoreceptor clones (GFP-negative) from an eye disc induced by *ey*>Gal4-UAS-Flp showed normal axon projections (red, anti-24B10) into a $babo^{52}$ heterozygous brain lobe. Anti-Elav antibody labeled differentiated neurons (magenta). (**F**) Expression of the 1407 Gal4 driver in the brain lobe is highlighted in green (anti-β-gal) and neurons in red (anti-Elav). Note the lack of *lacZ* staining in the eye disc and prominent staining of central brain neuroblasts (arrowhead) and the OPCs. (**G**) Expression of both UAS-$babo_{a+b}$ by the 1407 driver rescued the $babo^{26/32}$ mutant phenotype. Photoreceptor axons are in green (anti-24B10) and glia are in red (anti-Repo). (**H**) Expression of nuclear-GFP with the Wor>Gal4 driver is specific to neuroblasts and GMCs (arrowheads). Neurons are stained with Elav. Note the absence of GFP in the eye disc. The smaller OPC and IPC neuroblasts are not evident in this picture. (For additional images of Wor-Gal4 expression, see Fig. S3A-D in the supplementary material.) (**I**) Expression of both UAS-$babo_{a+b}$ by the *wor*>Gal4 rescues the $babo^{26/32}$ mutant phenotype. Photoreceptor axons are in green (anti-24B10) and neurons in red (anti-Elav). ed, eye disc; la, lamina.

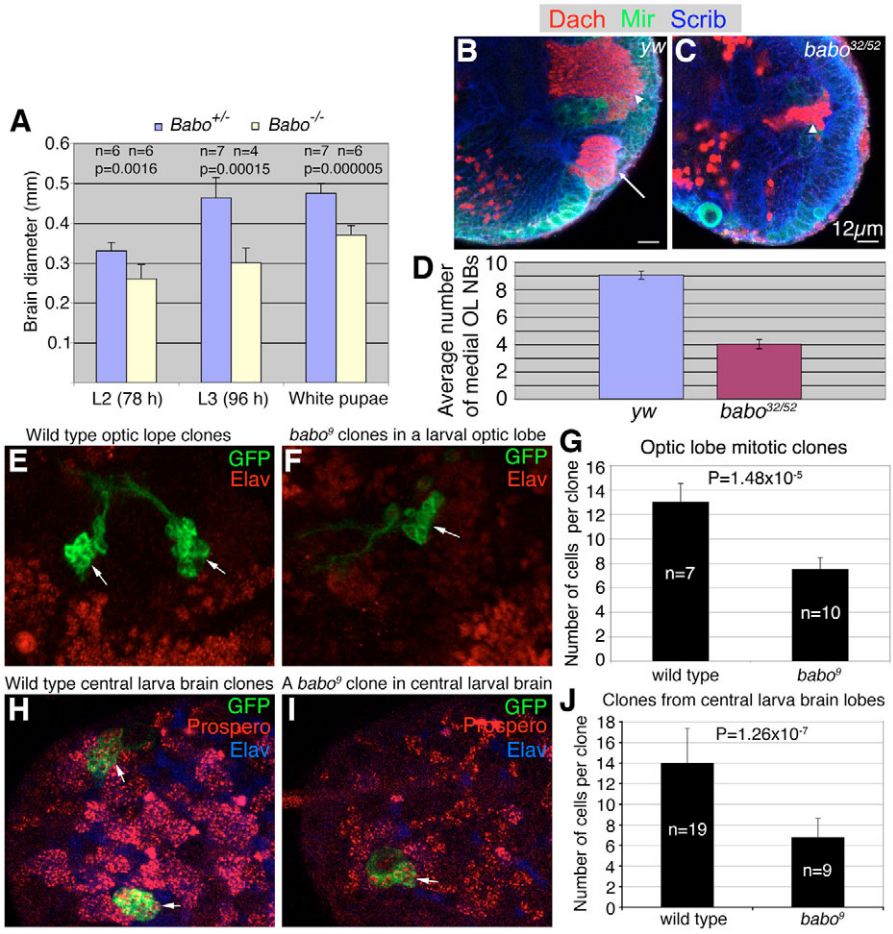

Fig. 4. Characterization of brain lobe size and proliferation rate of neuroblasts in *Drosophila babo* mutant larvae. (**A**) Brain lobe size as a function of larval stage. Larvae were dissected in PBS, mounted without coverslips, and brain lobe diameter was measured using a calibrated reticule. *P*-value is from Student's *t*-test. Error bars are standard deviation. (**B**,**C**) White prepupa (wpp) brain lobes of either wild type (B) or *babo*$^{32/52}$ mutant (C) were labeled by anti-Dachshund (red), anti-Miranda (green) and anti-Scribbled (blue) antibodies. (B) One half wild-type wpp optic lobe; anterior is up, posterior is down, lateral is right and medial is left. Scrib outlines all cell cortices in the wpp optic lobe; Mir marks medial neuroblasts of the optic lobe; Dach marks LPCs (arrow) and central plug progenitor cells from the IPC (arrowhead). (C) Three-quarters of a much smaller *babo*$^{32/52}$ wpp optic lobe. Much of the optic lobe remains primitive neuroepithelial cells indicative of a younger optic lobe [Scrib^{+}, Mira^{-} and Deadpan (Dpn), data not shown]. Dach marks the first progenitors to be born from the IPC (arrowhead). (**D**) Quantification of the average number of medial optic lobe (OL) neuroblasts (Nbs) per optic section of wandering third-instar larva brain (11 sections on left and right lobes for a total of 22 sections). On average, about 8-10 Miranda-positive optic lobe neuroblasts are seen per inner optic section of wild-type control brain lobes, whereas babo mutants have only about 4 Miranda-positive optic lobe neuroblasts per section. (**E-G**) MARCM clonal analysis of wild-type clones (arrows in E) or a *babo* mutant clone (arrow in F) 48 hours after heat shock. Brain lobes were stained by anti-Elav antibody (red). Mutant or wild-type clones are marked by GFP expression. The number of cells in well-defined clones within the optic lobes were counted and the quantification is shown (G). (**H-J**) MARCM clonal analysis of the proliferation rates of wild-type central larval brain neuroblasts (arrows in H) or a *babo*^{9} mutant central brain neuroblast clone (arrow in I) 48 hours after heat shock. Larval brain lobes were stained with anti-Prospero antibody (red) and anti-Elav antibody (blue). (J) Quantification of cell numbers derived from individual central brain neuroblasts.

differentiate properly. Instead, the defect in innervation may arise from the production of too few target field cells, perhaps as a result of proliferation defects within the optic lobe.

babo mutants have reduced numbers of optic lobe progenitors

babo mutant brain lobes are 25-40% smaller than *babo* heterozygous brain lobes throughout third-instar life (Fig. 4A). Previously, we have shown that *babo* mutant brain lobes do not exhibit an increase in apoptosis, suggesting that the small size of *babo* brains probably results from reduced proliferation and not cell death (Brummel et al., 1999). However, it is not clear how proliferation is affected in *babo* mutant brains. Because the optic lobes comprise the majority of brain lobe tissue, and have been well characterized (Egger et al., 2007), we focus on the growth and proliferation of the optic lobe.

In wild-type white prepupae, optic lobes make up more than half of the brain lobe. At late stages, the optic lobe epithelium produces many medulla neuroblasts and laminar precursor cells (LPCs). These neuroepithelial cells of the outer proliferation center (OPC) and inner proliferation center (IPC), as well as medulla neuroblasts and LPCs, undergo rapid proliferation to produce the cells of the lamina and medulla cortices (Fig. 4B) (Egger et al., 2007). As noted above, in *babo* mutants the optic lobe is much smaller than in wild-type controls. We find that the overall organization of the OPC and IPC epithelia is normal and that they retain their ability to produce neuroblasts and LPCs. However, there is approximately a 50% decrease in the number of medulla neuroblasts (Fig. 4D), a decrease in the number of ganglion mother cells produced from these medulla neuroblasts, and a subsequent decrease in the number of Elav^{+} maturing neurons within the medulla cortex (Fig. 4B,C). Furthermore, there is a decrease in the number of LPCs and thus a decrease in the number of lamina cartridges and laminar neurons (Fig. 2B and Fig. 4C, and see Fig. S2B,C in the supplementary material). Similar results are observed for central brain neuroblasts, where we observed a slight reduction in neuroblast numbers (see Fig. S2A in the supplementary material). We observed no evidence for an increase in apoptosis, as revealed by staining for Caspase-3 (also known as Decay – FlyBase) (Fig. 5N-P), confirming previous results (Brummel et al., 1999). We conclude that *babo* function is required for generating the normal number of medulla neuroblasts and laminar precursor cells in the optic lobe.

Neuroblasts proliferate more slowly in *babo* mutants

To further address whether proliferation rates are altered in *babo* mutant optic lobes, we generated GFP-positive marked *babo* loss-of-function clones using the MARCM system (Lee and Luo, 2001). As

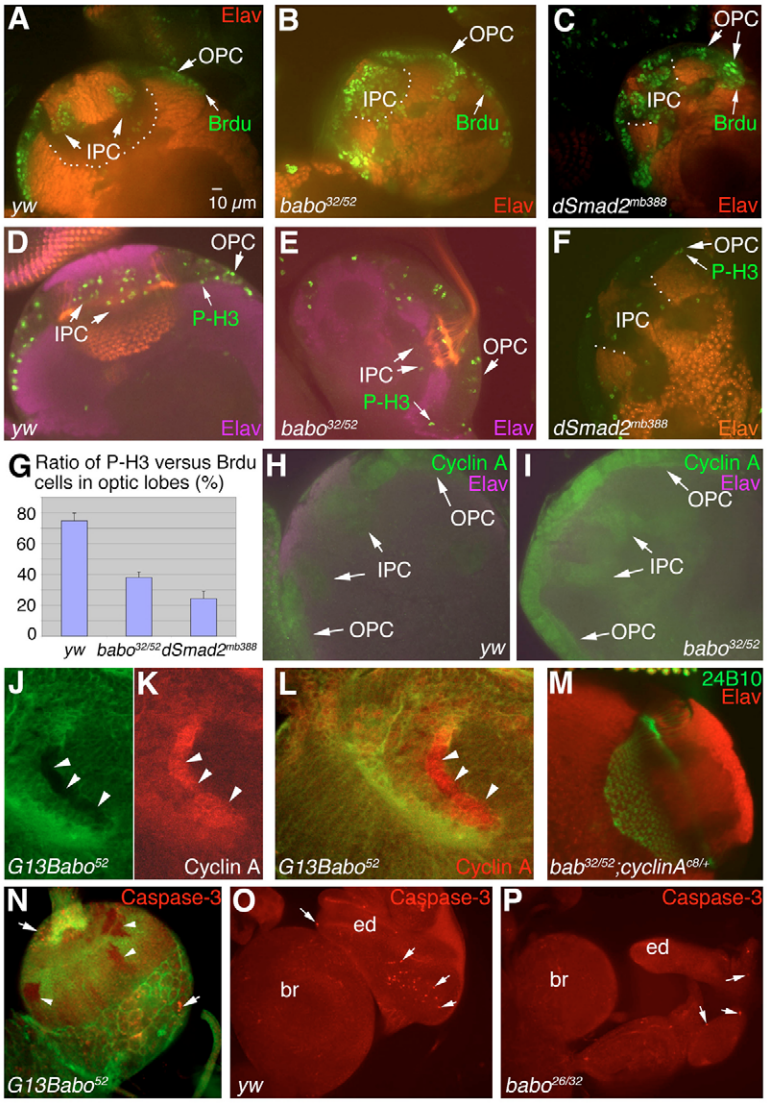

Fig. 5. *babo* mutants display cell cycle progression defects. S-phase cells (arrows) within the developing optic lobes of a wandering third-instar *yw Drosophila* larva (**A**) or *babo*$^{32/52}$ mutant (**B**) or *Drosophila Smad2* (*dSmad2*^{mb388}) (**C**) mutant were labeled with BrdU (green). M-phase cells in optic lobes of wandering third-instar larvae of wild type *yw* (**D**) and *babo*$^{32/52}$ mutant (**E**) and *Smad2*^{mb388} mutant (**F**) revealed by staining with phosphorylated histone H3 antibody (green, p-H3). Differentiated neurons are labeled by anti-Elav staining (A-F, magenta or red). Photoreceptor axons in red are labeled by 24B10 antibody (D,E). (**G**) Comparison of the ratio of M-phase cells versus S-phase cells in the optic lobes of *yw*, *babo*$^{32/52}$ mutant and *Smad2*^{mb388} mutants. BrdU-positive cells or p-H3 positive cells were counted from three individual and distinct optic sections at roughly the same plane of each optic lobe of the three genotypes. The ratio of p-H3 positive cells versus BrdU-positive cells was calculated for each genotype and compared. Note that both *babo*$^{32/52}$ and *Smad2*^{mb388} mutants showed a much reduced ratio of p-H3 positive cells to BrdU-positive cells compared with that of *yw* control. (**H**) Normal expression level of Cyclin A protein is seen in both IPC and OPC of an optic lobe of a *yw* third-instar larva. (**I**) High level Cyclin A protein is present at the optic center of a *babo*$^{32/52}$ mutant third-instar larva in both IPC and OPC stained and photographed with the same setting as wild type. (**J-L**) Elevated Cyclin A protein (red, arrowheads in K) is detected in a GFP-negative *babo*^{52} mutant clone (arrowheads in J) induced by heat shock from the optic lobe of *babo*$^{52/+}$ heterozygote larva brain. (L) Merged image of J and K. (**M**) Heterozygosity for *Cyclin* A rescues *babo*$^{32/52}$ photoreceptor axon targeting and lamina neuron phenotypes. (**N**) Anti-active Caspase-3 antibody staining (red) of *babo*^{52} mutant GFP-negative clones (arrowheads) in an otherwise *babo*^{52} heterozygous GFP-positive developing larval brain lobe. Caspase-3-positive apoptotic cells are indicated by arrows. (**O**,**P**) Apoptotic cells (arrows) identified by anti-active Caspase-3 antibody staining (red) of a *yw* wandering third-instar brain lobe and eye disc (O) compared to a *babo*$^{26/32}$ mutant brain (P). Note that there is no overall increase in the number of apoptoic cells in the *babo* mutant tissue. br, brain lobe; ed, eye disc.

there are different patterns of mitotic clones within the developing optic lobes (data not shown), we sought to compare only the *babo* mutant and wild-type clones at similar positions within the optic lobe (example clones in Fig. 4E vs F) and central brain (Fig. 4H vs I). This analysis revealed that *babo* mutant clones in the optic centers and central brain contained 30-50% fewer cells than did wild-type control clones, which agrees with the overall reduction of brain size and lamina cartridge size. We conclude that *babo* mutants have reduced proliferation of optic lobe and central brain neuroblasts.

Lack of Babo/Smad2 signaling slows the S-to-M cell cycle progression in the optic lobe, probably through accumulation of excess Cyclin A

We next investigated whether proliferation was affected by using BrdU and phospho-histone H3 (P-H3) labeling to identify cells in the S and M phase of the cell cycle, respectively. As shown in Fig. 5, wandering third-instar larvae of *babo*$^{32/52}$ and *Smad2*^{mb388} mutants exhibited many S-phase cells in both the OPC and IPC, as revealed by BrdU incorporation, although the sizes of these zones were reduced compared with wild type (Fig. 5A vs B,C). By contrast, the number of cells in M phase was significantly reduced compared with wild type (Fig. 5D vs E,F), resulting in an alteration of the M:S ratio in *babo* mutant brains (Fig. 5G). This suggests that loss of *babo*/*Smad2* signaling delays the transition from S-to-M phase of the cell cycle within the optic lobe. By contrast, *babo* mutant eye discs did not show a significant decrease in the size of the disc or number of cells in M phase, although we did observe ectopic M-phase cells within the morphogenetic furrow (see Fig. S1A vs B in the supplementary material), similar to the previously reported *dpp* mutant phenotype (Horsfield et al., 1998; Penton et al., 1997).

We next examined the levels of different Cyclins in *babo* mutant clones and fully mutant brains. We found no difference in the levels of Cyclin B and E (data not shown); however, Cyclin A levels were enhanced in both *babo* clones (Fig. 5J-L) and fully mutant brains (Fig. 5H,I). Ectopic expression of Cyclin A has been previously shown to accelerate the G1/S transition as well as delay cells from exiting M phase (Lehner and O'Farrell, 1989; Lehner et al., 1991; Sprenger et al., 1997). Thus, elevated Cyclin A in the *babo* mutants could lead to the observed decrease in M-phase cells. Consistent with this model, heterozygosity for the *Cyclin A*^{c8RL1} mutation substantially suppressed the *babo* mutant phenotype (Fig. 5M). We conclude that loss of Babo/Smad2 signaling leads to elevated Cyclin A levels, which contribute to the optic lobe proliferation defects seen in *babo* mutants.

actβ and *daw* act redundantly to regulate optic lobe development

Previous work has demonstrated that both *Drosophila* Activin-β and the Activin-like protein Dawdle signal through Activin type I receptor Babo to Smad2 (Zheng et al., 2003; Parker et al., 2006; Serpe and O'Connor, 2006), suggesting that one or both are likely candidates for regulating optic lobe development. In situ hybridization studies revealed that both are expressed in the developing optic lobes (Fig. 6A,B). In addition, *daw* is also expressed in many glial cells, including surface glia within the optic lobe, and Actβ is expressed in mushroom body neurons (Fig. 6C) (Serpe and O'Connor, 2006) (and data not shown).

To functionally characterize the role of the *actβ* and *daw* genes in larval optic lobe development, an EMS-induced $act\beta^{ed80}$ mutant was identified in a screen for fourth chromosome lethal mutations (S.H., L.P. and J.L., unpublished). This mutant line carries a stop codon (W 711 stop) within the prodomain N-terminal before the maturation cleavage site and is a presumed null allele. A large fraction of the $act\beta^{ed80}$ homozygous mutants survived to the pharate adult stage and a small proportion (<2%) eclosed. The escaper flies could not move their wings, walked very slowly and did not establish a breeding stock. As the mutation is rescued by expression of a UAS-*actβ* transgene, we conclude that there are no other lethal mutations on the $act\beta^{ed80}$ chromosome. As shown in Fig. 6F, these mutants exhibited normal optic lobe size and photoreceptor axon projections.

We also examined several *daw* mutant lines for optic lobe morphology. We observed no photoreceptor axon-targeting defects in daw^{3}/daw^{4} heteroallelic mutant larvae or the daw^{ex11} homozygous larvae (data not shown). However, in a low percentage (4%, *n*=50) of daw^{ex32} homozygous deletion mutants (Fig. 6D), we did observe photoreceptor axon targeting and optic lobe defects in white prepupae that were reminiscent of those seen in *babo* mutants (Fig. 6E). The low penetrance of the *babo*-like phenotypes in *daw* mutants, and the overlapping expression of *actβ* and *daw* in the optic lobes, suggested that these two genes might act redundantly to control growth in the optic lobes. To investigate this issue, we examined the phenotypes of various *daw, actβ* double mutant combinations. In the daw^{ex11}/daw^{ex11}, $act\beta^{ed80}/act\beta^{ed80}$ double mutants overall brain morphology was relatively normal. However, approximately 20% (*n*=30) of the mutant larvae exhibited collapsed and bundled R7 and 8 growth cones that were not seen in either single mutant (Fig. 6G). In the stronger daw^{ex32}/daw^{ex32} $act\beta^{ed80}/act\beta^{ed80}$ allelic combination, the penetrance of the severe small brain and axon-targeting phenotype seen in daw^{ex32} mutants alone was increased from 4 to 50% (*n*=30). In the daw^{4}/daw^{ex32}, $act\beta^{ed80}/act\beta^{ed80}$ combination, larvae died during late second- or early third-instar stages, precluding us from examining the brain phenotype. We conclude that Actβ and Daw function redundantly to control proliferation in the optic centers of the *Drosophila* larval brain.

DISCUSSION

In this report, we have demonstrated that an Activin-like signal is essential for proper development of the *Drosophila* brain. Specifically, this pathway is important for establishing the correct number of central brain and optic lobe neuroblasts and stimulating their proliferation. This reflects a direct requirement for reception of Activin signals in neuroblasts, as re-expression of the Activin receptor specifically in neuroblast lineages of *babo* mutant animals largely rescues the proliferation defects of the entire brain.

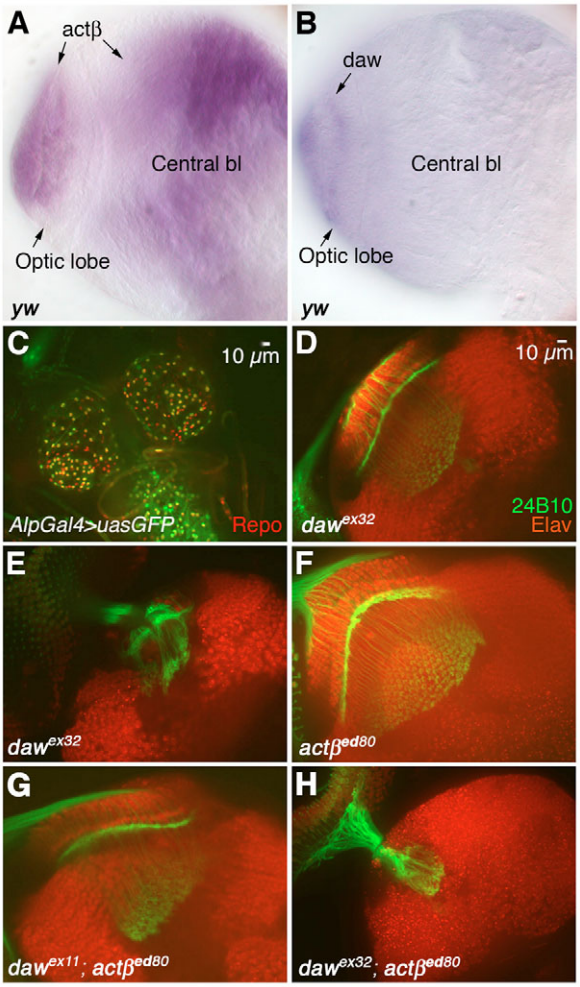

Fig. 6. Activin and Activin-related (*daw*) genes are expressed in developing larval optic lobes and required for normal optic lobe development and correct photoreceptor axon targeting in *Drosophila*. (**A**,**B**) In situ hybridization of wild-type *yw* mid-third-instar larval brain lobes with antisense probes of *activin-β* (A) and *daw* (B). The transcripts of *actβ* are abundantly expressed in both larval optic lobe and the central brain lobe, whereas *daw* gene is also expressed in the larval optic lobe (arrow) in addition to its known expression in glial cells. (**C**) A *daw* promoter-enhancer Gal4 transgene drives the expression of a uasGFP reporter in glia cells (green and yellow) in the developing larval brain lobes. Glial cells were stained by an anti-Repo antibody (red). (**D**) The majority (95%) of homozygous daw^{ex32} wandering third-instar larvae do not show abnormal optic lobe development or photoreceptor axon targeting defects. (**E**) A minority (~5%) of daw^{32} homozygotes show optic lobe and axon targeting defects reminiscent of babo mutants. (**F**) Optic lobes developed normally and photoreceptor axons target correctly in $act\beta^{ed80}$ mutant larvae. (**G**) Double mutants of the genotype daw^{ex11}:$act\beta^{ed80}$ exhibit altered R7 and R8 growth cone bundling and morphology. (**H**) The daw^{ex32};$act\beta^{ed80}$ double mutants showed significantly enhanced penetrance of the strong optic lobe phenotype. Central bl, central brain lobe.

It is not entirely clear how Activin signaling in neuroblast lineages maintains the wild-type number of brain neuroblasts. Approximately 100 neuroblasts per brain lobe are formed during embryogenesis, and most go quiescent at the embryonic/larval transition. From L1-L3 they progressively re-enter the cell cycle to resume their cell lineages. Perhaps the slower cell cycle of Activin pathway mutants

inhibits exit from quiescence and promotes premature differentiation. Mutations in *trol*, which encodes a heparin sulfate proteoglycan Perlecan, prevent neuroblast reactivation and lead to a severe reduction in neuroblast numbers and brain size (Datta, 1995; Park et al., 2003). Many TGF-β ligands bind to heparin sulfate proteoglycans, and thus part of the effect of Activin signaling on brain size might be mediated by Perlecan or other proteoglycans such as the glyipican Dally (see below).

The small brain size is not just caused by a reduced number of neuroblasts, however; *babo* mutant clones that contained a single neuroblast produced fewer daughter cells in a given time window than did wild-type neuroblasts, presumably due to the increased expression of Cyclin A and the delay in metaphase exit. One additional possibility is that the Activin signal may affect neuroblast temporal identity progression in larval neuroblast lineages, similar to the effect of temporal identity mutations on embryonic neuroblast lineages (Isshiki et al., 2001), leading to the failure to produce early, mid or late subsets of larval lineages. Testing this hypothesis awaits the development of markers for different neurons within optic lobe neuroblast lineages.

The importance of Activin in regulating neuroblast proliferation is reminiscent of the positive role that Activin/Nodal signaling plays in regulating the cell cycle of mouse and human ES cells (James et al., 2005; Ogawa et al., 2006). In those cells, as in *Drosophila* neuroblasts, Activin/Nodal signaling enhances, but is not absolutely required for, cell proliferation (Ogawa et al., 2006). Another point of potential similarity is that the mES cells endogenously produce an Activin/Nodal signal leading to an autocrine/paracrine regulation of proliferation. While our in situ data are not of sufficient resolution to unambiguously assign expression of *actβ* and *daw* to particular cell types, both are expressed in the optic proliferation zones where neuroblasts are highly concentrated. It is also possible that some ligand may be supplied by the innervating photoreceptors. Activin is strongly expressed in R7 and 8 (Ting et al., 2007) and like *hh* and *spitz* may provide a tropic signal that simulates proliferation in the target tissue (Huang and Kunes, 1996; Huang et al., 1998).

Lastly, it is interesting to note that Activins are not the only TGF-β-like factors required for proliferation of *Drosophila* neuroblasts. The BMP family member Dpp is expressed in four regions in each brain lobe (Kaphingst and Kunes, 1994; Yoshida et al., 2005). Two lie in the dorsal and ventral margins of the posterior optic zone neuroepithelium near what has been termed the lamina glial precursor region (Yoshida et al., 2005), whereas the other two smaller zones are more interior at the base of the inner proliferation zone. In the brain, the *dpp* loss-of-function phenotype is remarkably similar to that seen in *babo* mutants (Kaphingst and Kunes, 1994; Yoshida et al., 2005). A potential trivial explanation for the similarity in phenotypes might be that Activin signaling is required for *dpp* expression, or vice versa. However, *dpp* is still expressed in *babo* mutants (see Fig. S1C,D in the supplementary material) and *daw* and *actβ* are both still expressed in *dpp* mutants, although it is difficult to know in each case whether the levels are equivalent. Thus, both Dpp and Activin signaling appear to be required to stimulate brain neuroblast proliferation.

In addition to regulating proliferation in the brain, Dpp signaling plays a major role in regulating proliferation in other tissues, including the imaginal discs (Burke and Basler, 1996; Rogulja and Irvine, 2005). Once again, Activins may collaborate with BMPs in regulating proliferation in this tissue. In particular, we note that *babo* mutants show ectopic P-H3 staining within the morphogenetic furrow of the eye disc, which is also observed in loss-of-function mutants in the Dpp receptor Tkv (Horsfield et al., 1998). Furthermore, *babo* mutant wing disc clones can grow large in contrast to clones mutant in *dpp* signaling components (Burke and Basler, 1996), although the overall sizes of *babo* mutant discs are not affected proportionally as much as is the brain (C.C.Z. and M.B.O., unpublished). Therefore, the way in which BMP and Activin inputs regulate the cell cycle might be different in discs versus the brain, or the two tissues might exhibit different sensitivities to common inputs.

How Activins and BMPs affect the cell cycle is not entirely clear. In the wing disc, Dpp signaling through Tkv/Mad has been shown to promote the G1-S transition (Martin-Castellanos and Edgar, 2002). In the brain, *babo* mutants exhibit a decrease in the M/S ratio, which could be due to a decrease in cells at the G2/M phase of the cell cycle. Consistent with this view, we find that Cyclin A levels are enhanced in *babo* mutants and that heterozygosity for a *Cyclin A* mutation suppresses the *babo* phenotype. This is very similar to that seen in *dally* mutants, which also affect brain development by causing a delay in the G2-M transition within the outer proliferation centers. Just as we have found for *babo* mutants, heterozygosity for *Cyclin A* suppresses the *dally* cell cycle defect (Nakato et al., 2002).

Given the results described above, one attractive model for how both BMPs and Activins contribute to cell cycle progression is that they regulate the cycle at different points: Activins at G2-M and BMPs at G1-S. Alternatively, as previous work has suggested that Cyclin A probably has roles in regulating both G2-M and G1-S transitions in *Drosophila* (Lehner and O'Farrell, 1989; Lehner et al., 1991; Sprenger et al., 1997) and as Smads can form heterotrimers (Chacko et al., 2004), it may be that a composite signal composed of a Smad2/Mad/Medea heterotrimer acts at several points in the cell cycle. Interestingly, several potential target genes that are regulated by both Activin and BMP signals in the larval brain have been identified by microarray studies using activated receptors (Yang et al., 2004), but no obvious candidates for genes that might influence proliferation are evident within the list.

Lastly, we note that *daw* has been demonstrated previously to play a role in motoneuron axon guidance in the embryo, while *actβ* has been implicated in mushroom body remodeling (Zheng et al., 2003) and more recently in regulating the terminal steps in photoreceptor R8 targeting during pupal stages (Ting et al., 2007). As both ligands are expressed in each of these tissues (P.A.J. and M.B.O., unpublished), it is possible that there may be functional redundancy that limits the severity of the previously observed phenotypes. Consistent with this view, we have recently found that both *actβ* and *daw* modulate neurotransmission at the neuromuscular junction and that the double mutant phenotypes are more severe than those seen in the single mutants (Yi Ren and M.B.O., unpublished), similar to their redundant function in regulating neuroblast proliferation described here. In conclusion, all available data suggest that Activin signaling plays at least two important roles in *Drosophila* nervous system development. First, it ensures that the proper numbers of cells are produced in the CNS; and second, it helps establish correct functional connections between neurons and their synaptic partners.

We thank Thomas Neufeld, and Hiroshi Nakato for anti-Cyclin E and anti-Cyclin A antibodies, and also for comments on the manuscript. Anti-N-Cadherin was generously provided by Larry Zipursky. We thank Karl-Friedrich Fischbach and Vanessa J. Auld for fly lines, Mary Jane Shimell for *actβ* and *daw* in situ hybridization, and Ying Li for examining *dpp* mRNA expression in *babo* mutants. J.Q.B. was supported by a NSF IGERT pre-doctoral training grant. M.B.O. and C.Q.D. are Investigators of the Howard Hughes Medical Institute.

Supplementary material

Supplementary material for this article is available at http://dev.biologists.org/cgi/content/full/135/3/513/DC1

References

Albertson, R., Chabu, C., Sheehan, A. and Doe, C. Q. (2004). Scribble protein domain mapping reveals a multistep localization mechanism and domains necessary for establishing cortical polarity. *J. Cell Sci*. **117**, 6061-6070.

Barolo, S., Carver, L. A. and Posakony, J. W. (2000). GFP and beta-galactosidase transformation vectors for promoter/enhancer analysis in Drosophila. *Biotechniques* **29**, 726, 728, 730, 732.

Brummel, T. J., Twombly, V., Marques, G., Wrana, J. L., Newfeld, S. J., Attisano, L., Massague, J., O'Connor, M. B. and Gelbart, W. M. (1994). Characterization and relationship of Dpp receptors encoded by the *saxophone* and *thick veins* genes in Drosophila. *Cell* **78**, 251-261.

Brummel, T., Abdollah, S., Haerry, T. E., Shimell, M. J., Merriam, J., Raftery, L., Wrana, J. L. and O'Connor, M. B. (1999). The Drosophila activin receptor baboon signals through dSmad2 and controls cell proliferation but not patterning during larval development. *Genes Dev*. **13**, 98-111.

Burke, R. and Basler, K. (1996). Dpp receptors are autonomously required for cell proliferation in the entire developing Drosophila wing. *Development* **122**, 2261-2269.

Chacko, B. M., Qin, B. Y., Tiwari, A., Shi, G., Lam, S., Hayward, L. J., De Caestecker, M. and Lin, K. (2004). Structural basis of heteromeric smad protein assembly in TGF-beta signaling. *Mol. Cell* **15**, 813-823.

Clandinin, T. R. and Zipursky, S. L. (2002). Making connections in the fly visual system. *Neuron* **35**, 827-841.

Das, P., Inoue, H., Baker, J. C., Beppu, H., Kawabata, M., Harland, R. M., Miyazono, K. and Padgett, R. W. (1999). Drosophila dSmad2 and Atr-I transmit activin/TGFbeta signals. *Genes Cells* **4**, 123-134.

Datta, S. (1995). Control of proliferation activation in quiescent neuroblasts of the Drosophila central nervous system. *Development* **121**, 1173-1182.

Egger, B., Boone, J. Q., Stevens, N. R., Brand, A. H. and Doe, C. Q. (2007). Regulation of spindle orientation and neural stem cell fate in the Drosophila optic lobe. *Neural Dev*. **2**, 1.

Feng, X. H. and Derynck, R. (2005). Specificity and versatility in tgf-beta signaling through Smads. *Annu. Rev. Cell Dev. Biol*. **21**, 659-693.

Hidalgo, A., Learte, A. R., McQuilton, P., Pennack, J. and Zhu, B. (2006). Neurotrophic and gliatrophic contexts in Drosophila. *Brain Behav. Evol*. **68**, 173-180.

Horsfield, J., Penton, A., Secombe, J., Hoffman, F. M. and Richardson, H. (1998). decapentaplegic is required for arrest in G1 phase during Drosophila eye development. *Development* **125**, 5069-5078.

Huang, Z. and Kunes, S. (1996). Hedgehog, transmitted along retinal axons, triggers neurogenesis in the developing visual centers of the Drosophila brain. *Cell* **86**, 411-422.

Huang, Z. and Kunes, S. (1998). Signals transmitted along retinal axons in Drosophila: Hedgehog signal reception and the cell circuitry of lamina cartridge assembly. *Development* **125**, 3753-3764.

Huang, Z., Shilo, B. Z. and Kunes, S. (1998). A retinal axon fascicle uses spitz, an EGF receptor ligand, to construct a synaptic cartridge in the brain of Drosophila. *Cell* **95**, 693-703.

Isshiki, T., Pearson, B., Holbrook, S. and Doe, C. Q. (2001). Drosophila neuroblasts sequentially express transcription factors which specify the temporal identity of their neuronal progeny. *Cell* **106**, 511-521.

James, D., Levine, A., Besser, D. and Hemmati-Brivanlou, A. (2005). TGFß/Activin/Nodal signaling is necessary for the maintenacne of pluripotency in human embryonic stem cells. *Development* **132**, 1273-1282.

Kaphingst, K. and Kunes, S. (1994). Pattern formation in the visual centers of the Drosophila brain: wingless acts via decapentaplegic to specify the dorsoventral axis. *Cell* **78**, 437-448.

Lee, C. H., Herman, T., Clandinin, T. R., Lee, R. and Zipursky, S. L. (2001). N-cadherin regulates target specificity in the Drosophila visual system. *Neuron* **30**, 437-450.

Lee, C. Y., Andersen, R. O., Cabernard, C., Manning, L., Tran, K. D., Lanskey, M. J., Bashirullah, A. and Doe, C. Q. (2006). Drosophila Aurora-A kinase inhibits neuroblast self-renewal by regulating aPKC/Numb cortical polarity and spindle orientation. *Genes Dev*. **20**, 3464-3474.

Lee, T. and Luo, L. (2001). Mosaic analysis with a repressible cell marker (MARCM) for Drosophila neural development. *Trends Neurosci*. **24**, 251-254.

Lehner, C. F. and O'Farrell, P. H. (1989). Expression and function of Drosophila cyclin A during embryonic cell cycle progression. *Cell* **56**, 957-968.

Lehner, C. F., Yakubovich, N. and O'Farrell, P. H. (1991). Exploring the role of Drosophila cyclin A in the regulation of S phase. *Cold Spring Harb. Symp. Quant. Biol*. **56**, 465-475.

Letsou, A., Arora, K., Wrana, J. L., Simin, K., Twombly, V., Jamal, J., Staehling-Hampton, K., Hoffmann, F. M., Gelbart, W. M., Massague, J. et al. (1995). Drosophila Dpp signaling is mediated by the punt gene product: a dual ligand-binding type II receptor of the TGF beta receptor family. *Cell* **80**, 899-908.

Luo, L., Liao, Y. J., Jan, L. Y. and Jan, Y. N. (1994). Distinct morphogenetic functions of similar small GTPases: Drosophila Drac1 is involved in axonal outgrowth and myoblast fusion. *Genes Dev*. **8**, 1787-1802.

Martin-Castellanos, C. and Edgar, B. A. (2002). A characterization of the effects of Dpp signaling on cell growth and proliferation in the Drosophila wing. *Development* **129**, 1003-1013.

Massague, J., Blain, S. W. and Lo, R. S. (2000). TGFbeta signaling in growth control, cancer, and heritable disorders. *Cell* **103**, 295-309.

Miyazono, K., Maeda, S. and Imamura, T. (2006). smad transcriptional co-activators and co-repressors. In *Smad Signal Transduction*. Vol. 5 (ed. P. Ten Dijke and C.-H. Heldin), pp. 277-293. Heidelberg: Springer.

Nakato, H., Fox, B. and Selleck, S. B. (2002). dally, a Drosophila member of the glypican family of integral membrane proteoglycans, affects cell cycle progression and morphogenesis via a Cyclin A-mediated process. *J. Cell Sci*. **115**, 123-130.

Ogawa, K., Saito, A., Matsui, H., Suzuki, H., Ohtsuka, S., Shimosato, D., Morishata, Y., Watabe, T., Niwa, H. and Miyazono, K. (2006). Activin-nodal signaling is involved in propagation of mouse embryonic stem cells. *J. Cell Sci*. **120**, 55-65.

Park, Y., Rangel, C., Reynolds, M. M., Caldwell, M. C., Johns, M., Nayak, M., Welsh, C. J., McDermott, S. and Datta, S. (2003). Drosophila perlecan modulates FGF and hedgehog signals to activate neural stem cell division. *Dev. Biol*. **253**, 247-257.

Parker, L., Stathakis, D. G. and Arora, K. (2004). Regulation of BMP and activin signaling in Drosophila. *Prog. Mol. Subcell. Biol*. **34**, 73-101.

Parker, L., Ellis, J. E., Nguyen, M. Q. and Arora, K. (2006). The divergent TGF-beta ligand Dawdle utilizes an activin pathway to influence axon guidance in Drosophila. *Development* **133**, 4981-4991.

Penton, A., Selleck, S. B. and Hoffmann, F. M. (1997). Regulation of cell cycle synchronization by decapentaplegic during Drosophila eye development. *Science* **275**, 203-206.

Rogulja, D. and Irvine, K. D. (2005). Regulation of cell proliferation by a morphogen gradient. *Cell* **123**, 449-461.

Ruberte, E., Marty, T., Nellen, D., Affolter, M. and Basler, K. (1995). An absolute requirement for both the type II and type I receptors, punt and thick veins, for dpp signaling in vivo. *Cell* **80**, 889-897.

Serpe, E. and O'Connor, M. B. (2006). The metalloprotease Tolloid-related regulates Drosophila motoneuron axon guidance by activating latent TGF-β type ligands. *Development* **133**, 4969-4979.

Shimmi, O., Ralston, A., Blair, S. S. and O'Connor, M. B. (2005a). The crossveinless gene encodes a new member of the Twisted gastrulation family of BMP-binding proteins which, with Short gastrulation, promotes BMP signaling in the crossveins of the Drosophila wing. *Dev. Biol*. **282**, 70-83.

Shimmi, O., Umulis, D., Othmer, H. and O'Connor, M. B. (2005b). Facilitated transport of a Dpp/Scw heterodimer by Sog/Tsg leads to robust patterning of the Drosophila blastoderm embryo. *Cell* **120**, 873-886.

Sigrist, S. J. and Lehner, C. F. (1997). Drosophila fizzy-related down-regulates mitotic cyclins and is required for cell proliferation arrest and entry into endocycles. *Cell* **90**, 671-681.

Sprenger, F., Yakubovich, N. and O'Farrell, P. H. (1997). S-phase function of Drosophila cyclin A and its downregulation in G1 phase. *Curr. Biol*. **7**, 488-499.

Tayler, T. D., Robichaux, M. B. and Garrity, P. A. (2004). Compartmentalization of visual centers in the Drosophila brain requires Slit and Robo proteins. *Development* **131**, 5935-5945.

Ting, C.-Y., Herman, T., Yonekura, S., Gao, S., Wang, J., Serpe, M., O'Connor, M. B., Zipursky, L. and Lee, C.-H. (2007). Tiling of R7 in the Drosophila visual system is mediated both by transduction of an Activin signal to the nucleus and by mutual repression. *Neuron* **56**, 793-806.

Whitfield, W. G., Gonzalez, C., Maldonado-Codina, G. and Glover, D. M. (1990) The A- and B-type cyclins of Drosophila are accumulated and destroyed in temporally distinct events that define separable phases of the G2-M transition. *EMBO J.* **9**, 2563-2572.

Wrana, J. L., Tran, H., Attisano, L., Arora, K., Childs, S. R., Massague, J. and O'Connor, M. B. (1994). Two distinct transmembrane serine/threonine kinases from Drosophila melanogaster form an activin receptor complex. *Mol. Cell. Biol*. **14**, 944-950.

Yang, M., Nelson, D., Funakoshi, Y. and Padgett, R. W. (2004). Genome-wide microarray analysis of TGFbeta signaling in the Drosophila brain. *BMC Dev. Biol*. **4**, 14.

Yoshida, S., Soustelle, L., Giangrande, A., Umetsu, D., Murakami, S., Yasugi, T., Awasaki, T., Ito, K., Sato, M. and Tabata, T. (2005). DPP signaling controls development of the lamina glia required for retinal axon targeting in the visual system of Drosophila. *Development* **132**, 4587-4598.

Zheng, X., Wang, J., Haerry, T. E., Wu, A. Y.-H., Martin, J., O'Connor, M. B., Lee, C.-H. and Lee, T. (2003). TGF-ß signaling activates steroid hormone receptor expression during neuronal remodeling in the *Drosophila* brain. *Cell* **112**, 303-315.

Zheng, X., Zugates, C. T., Lu, Z., Shi, L., Bai, J. M. and Lee, T. (2006). Baboon/dSmad2 TGF-beta signaling is required during late larval stage for development of adult-specific neurons. *EMBO J.* **25**, 615-627.